

## Directive and Broadband 4-seg SRR Metamaterial Antennas

Parul Dawar<sup>1</sup>, Asok De<sup>2</sup> and N. S. Raghava<sup>3</sup>

<sup>1</sup>Department of ECE, Guru Tegh Bahadur Institute of Technology, GGSIPU,  
Delhi, India

<sup>2</sup>Director, NIT Patna, Bihar, India

<sup>3</sup>Department of ECE, Delhi Technological University, Delhi, India

<sup>1</sup>paru.dawar@gmail.com, <sup>2</sup>asok.de@gmail.com, <sup>3</sup>nsraghava@gmail.com

### Abstract

*In this paper, a design of novel Mu Negative Group (MNG) 4segment SRR based microstrip patch antenna optimized for bandwidth, directivity and front to back lobe ratio has been presented. The microstrip patch antenna is designed using Ansoft HFSS version 13. Results were compared with MATLAB programming based on CAD formulas using equivalent circuit analysis of patch antenna. Nicolson Ross Weir (NRW) method has been used to retrieve the material parameters from transmission and reflection coefficient. Following this, a metamaterial-based-microstrip patch antenna has been designed. The unique shape proposed in this paper, gives remarkable enhancement in bandwidth by 30GHz, directivity by 2% and front to back lobe ratio by 9% but at cost of reducing antenna gain.*

**Keywords:** Antennas, metamaterials (MTMs), negative index material, negative refraction, RMPA, DNG, HFSS, MNG

## 1. Introduction

RMPA *i.e.*, Rectangular Microstrip Patch Antenna, as the name implies consists of a rectangular patch over a microstrip substrate. Its major disadvantage is relatively low-impedance bandwidth which limits the field of application of these antennas. This calls for a novel technique to increase the bandwidth of antenna without altering its parameters and without much affecting the antenna's radiation properties. Henceforth, metamaterial based antennas have been introduced [1]. The geometry of negative permittivity particle has a strong effect on its surface plasmonic properties [2]. The software tool HFSS version 13 is used for simulation because it is a high performance full wave electromagnetic (EM) field simulator for arbitrary 3D volumetric passive device modeling [3].

This paper abridges the design of RMPA, with design frequency 120 THz and operating range of 110 THz to 130 THz having RT Duroid ( $\epsilon_r=2.33$ ) as substrate material in Section 2 by using Finite Element Method based Ansoft HFSS software. Section 3 gives parametric study using equivalent circuit analysis in MATLAB for patch antenna. Section 4 describes MNG 4 segment SRR having negative refraction in the designed RMPA range. Section 5 shows the designing of metamaterial using equivalent circuits. Section 6 elucidates upon their application in antenna parameter optimization by embedding their array in the middle of the antenna substrate and just below the microstrip rectangular patch. Section 7 discusses the results and concludes the paper.

## 2. Designing of Patch Antenna in FEM based Ansoft HFSS Software

Transmission Line model represents RMPA as two slots of width,  $w$ , and height,  $h$ , separated by transmission line of length,  $l$ . So,  $L_{\text{eff}}$ , *i.e.*, effective length is defined which

is obtained by adding  $2\Delta l$  (additional length  $\Delta l$  due to fringing on each end) to the length obtained by using mathematical design equations [4]. Ground plane has length,  $l_g$ , and width,  $w_g$ .

Microstrip feed using quarter wave transformer has been used for feeding the antenna as calculated from equation 1. The input impedance is taken at the base of microstrip feedline and is referred to  $50\Omega$ . i.e.  $Z_0$ .

$$Z_{qw} = \sqrt{Z_{rmpa} * Z_0} \quad (1)$$

where the  $W_{qw}$  and  $L_{qw}$  represent the width and length of the quarter wave transformer as calculated from  $Z_{qw}$  i.e., impedance of quarter wave transformer using TX line software by AWR.

The operating frequency range of the RMPA designed for 4segment SRR MTM is from 110THz to 130THz with center frequency 120THz with RT Duroid ( $\epsilon_r = 2.33$ ) as substrate as shown in Figure 1.

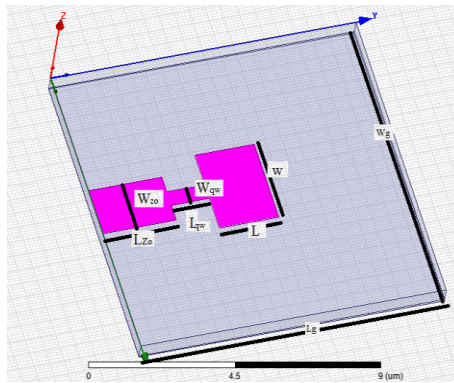


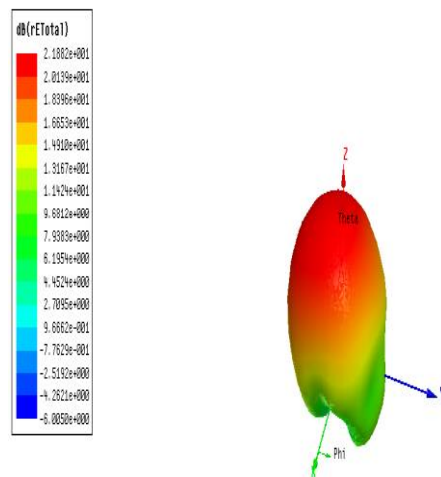
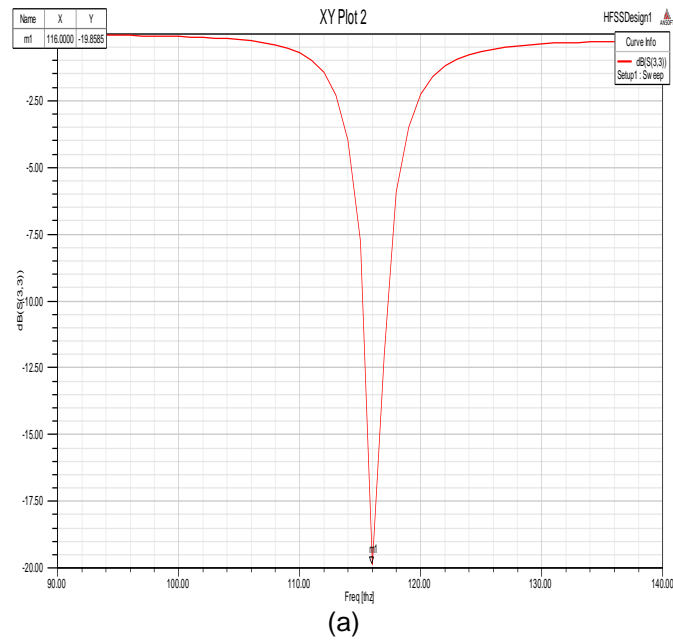
**Figure 1. Rectangular Microstrip Patch Antenna**

Constructional details are shown in Table 1.

**Table 1. Design Parameters of RMPA for 4-segment SRR MTM**

Frequency range	110-130 THz
Center frequency	120THz
$\epsilon_r$	2.33
$\epsilon_{eff}$	2.18
<b>h</b>	<b>50nm</b>
<b>w</b>	<b>969nm</b>
<b>L<sub>eff</sub></b>	<b>847nm</b>
<b><math>\Delta L</math></b>	<b>25.8nm</b>
<b>L</b>	<b>795nm</b>
<b>L<sub>g</sub></b>	<b>2000nm</b>
<b>W<sub>g</sub></b>	<b>2000nm</b>
<b>L<sub>qw</sub></b>	<b>427nm</b>
<b>W<sub>qw</sub></b>	<b>404nm</b>
<b>L<sub>zo</sub></b>	<b>442nm</b>
<b>W<sub>zo</sub></b>	<b>134nm</b>

RMPA has been simulated in HFSS. Figure 2 shows the simulation results where S11 is return loss or reflection coefficient.



(b)

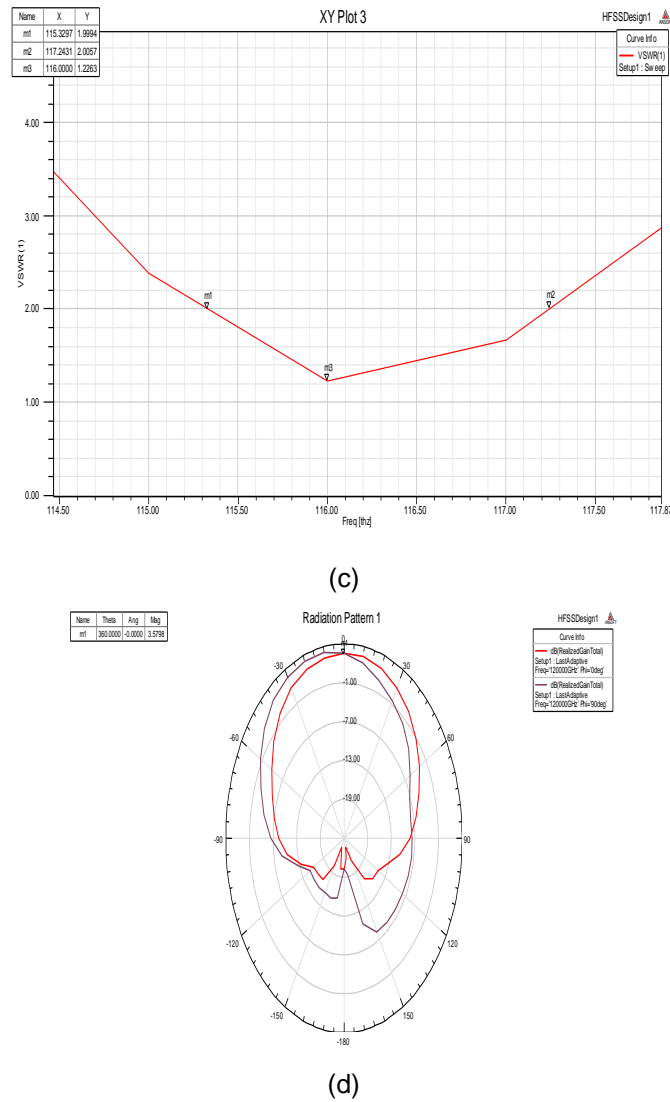


**Figure 2. a) Return Loss b) 3D Polar Plot c) VSWR d) Radiation Pattern in E and H Plane of RMPA**

Simulation results have been shown in Table 2.

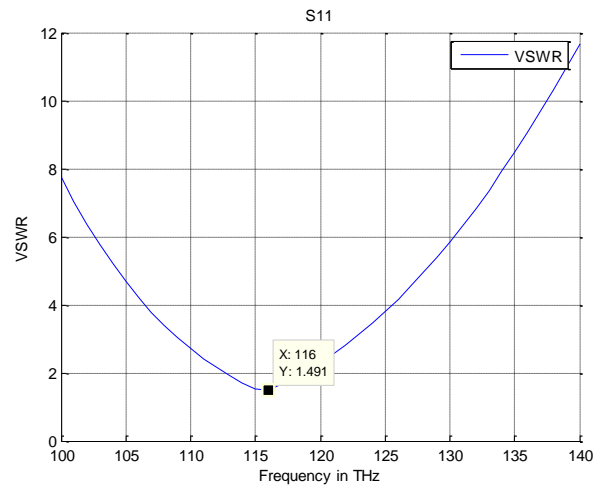
**Table 2. Simulation Results of RMPA at 116THz**

Parameters	RMPA
<b>S11 (dB)</b>	-19.86
<b>VSWR</b>	1.23
<b>Bandwidth (THz)</b>	1.91
<b>H plane gain in dB</b>	3.6
<b>E plane gain in dB</b>	3.6
<b>Peak directivity(dB)</b>	5.9
<b>Front to back lobe ratio</b>	32

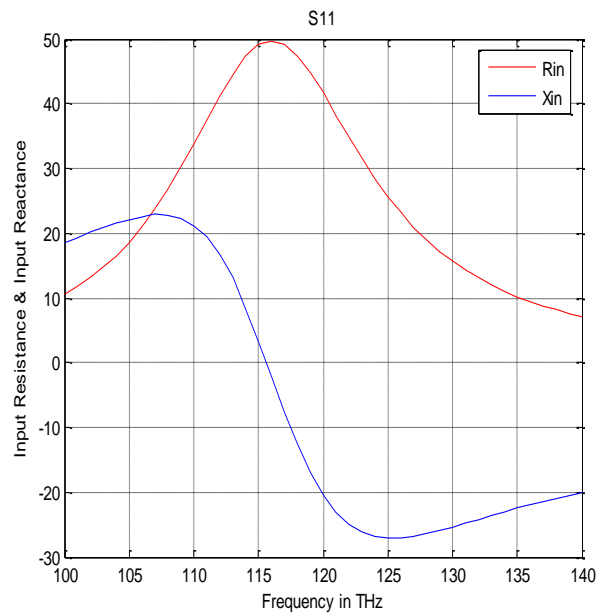
It can be seen that S11 is crossing 10 dB line and VSWR is less than 2. Bandwidth is 3.92 THz, which is range of frequencies with VSWR < 2.

### 3. Designing of Patch Antenna in MATLAB

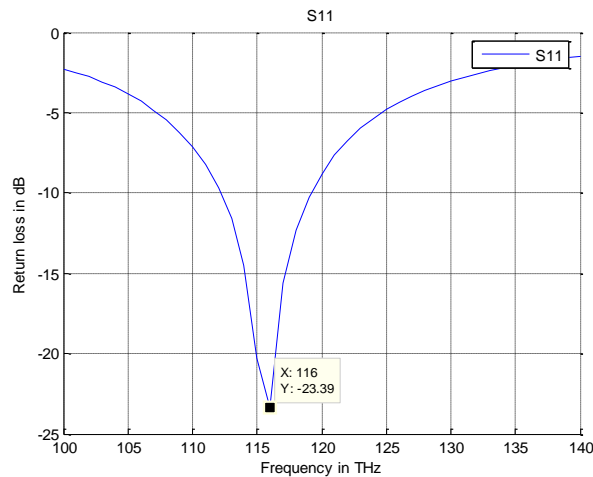
The parametric study of microstrip antennas using the CAD formulas is fairly accurate for thin substrates and illustrates the basic principles. For thin substrates the CAD formulas may even be accurate enough for final design purposes [5]. For thicker substrates these formulas can still be used for initial design work, with full-wave simulation tools used to complete the final design. Using CAD formulas and programming in MATLAB by parametric study, following results have been obtained in Figure 3.



(a)



(b)



(c)

**Figure 3. RMPA for '4seg' Shaped MTM: a) VSWR b) Input Impedance vs Frequency c) Return Loss**

It can be observed that using CAD formulas for microstrip patch antenna in MATLAB, we can initially plot the curve between input impedance and frequency. Thereby, we can obtain S11 and VSWR by applying the formulas,

Reflection coefficient is ratio of  $(Z_{in}-Z_0)/(Z_{in}+Z_0)$  and VSWR is ratio of  $(1+abs(reflection\ coefficient))/(1-abs(reflection\ coefficient))$ .

From the curve of VSWR, the percentage bandwidth can be calculated by the percentage difference of lower and upper frequency bounds with the centre frequency. Peak directivity can also be found using CAD formulas. The results obtained by coding in MATLAB have been shown in Table 3.

**Table 3. Simulation Results of RMPA using Matlab**

Parameters	Using Matlab	Using HFSS
S <sub>11</sub> (dB)	-23.39	-19.86
VSWR	1.491	1.23
%Bandwidth	4	2
Peak directivity(dB)	7.55	5.9

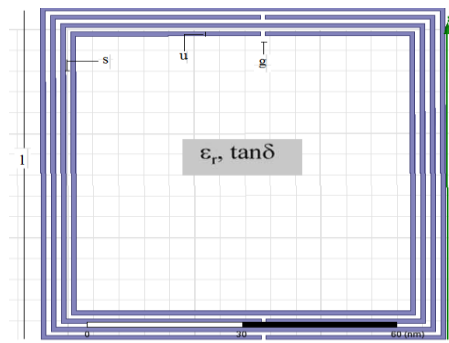
Thus, the results obtained from two different methods of analysis *i.e.*, CAD formulas in MATLAB and Finite Element Method in HFSS are differing with each other by nearly about 15%.

#### 4. 4-segment SRR Metamaterials

Multiple split ring (4 segment) metamaterial has been proposed having magnetic resonance. It behaves as MNG *i.e.*, Mu Negative Group. The wire strips affect the  $\epsilon$  and the split-ring resonators (SRRs) alter the  $\mu$  of the medium thus giving a frequency dependent negative material with both the parameters negative. The wire medium and the SRRs have certain frequency dependence. The rod gives negative permittivity,  $\epsilon$ , and ring material creates a negative permeability,  $\mu$ , this combined rod and ring material gives negative index of refraction [6-9].

Such materials have negative permeability over some frequency region [10], [11]. The parameter retrieval *i.e.*, parameter extraction using S parameters [12] has been followed using NRW approach to observe the negative refraction region of MTM.

It is construction ally very simple, consists of a 4 segment SRR with RT Duroid Substrate [13]. It is designed in such a way that the inclusions are much smaller than the operating wavelength. Such structures can be denoted by quasi-static equivalent LC circuit. Unit cell formed in HFSS is shown in Figure 4(a) , having metamaterial in the dielectric substrate bounded by box on either side having air as material and radiation boundary, .with constructional details in Figure 4(b) where thickness ‘t’ of the conducting metallic inclusions (N=4) is 0.08nm, height ‘h’ of the substrate is 2nm, conductivity ‘ps’ is  $0.017 \times 10^{-6} \Omega m$ , ‘l’ is the side length of the external ring, ‘u’ is the width of the strips, ‘s’ is the separation between two adjacent strips, ‘g’ is the gap width.



(a)

Parameter	Value (in nm)
<b>l</b>	<b>80</b>
<b>g</b>	<b>1</b>
<b>s</b>	<b>1</b>
<b>u</b>	<b>1</b>

(b)

**Figure 4. 4 Segment SRR MTM a) Unit Cell Designed in HFSS b) Constructional Details with  $\tan\delta=0.01$**

Nicolson Ross Weir (NRW) method has been used to calculate the material properties from transmission and reflection coefficients.

It can be observed as in Figure 5 that magnetic resonance is seen at 107.5054THz.

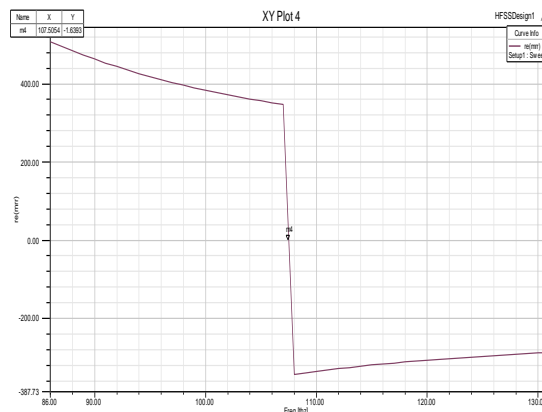


**Figure 5. Resonance in Permeability at 107.5054THz**

## 5. Designing of 4-segment SRR Metamaterials

4-segment SRR MTM has magnetic properties because of internal inductances and capacitances. It can be simplified in terms of combinations of parallel RC and series RL. Using transmission line theory (quasi-static regime), we can draw its equivalent circuit as in Figure 6(a), (b).

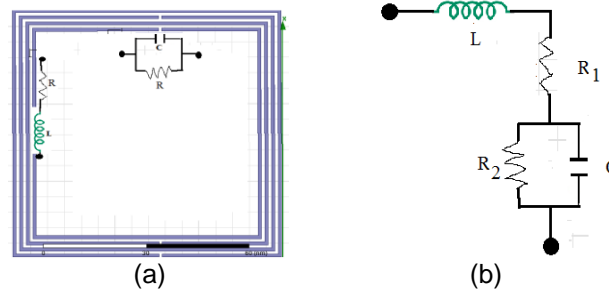


**Figure 6. (a), (b) Equivalent RLC Circuit of 4 Segment SRR**

The L is the inductance per unit length of the loop and C is the capacitance of the gap. Also, series resistance R1 is to take into account the losses in the conductor and a shunt resistance R2 is taken to describe the losses in the dielectric substrate as shown in figure 6(b).

The expressions for L and C are given by equation 2 and 3 as below [14]:

$$L = \frac{\mu_0}{2} \frac{l_{avg}}{4} 4.86 \left[ \ln \left( \frac{0.98}{\rho} \right) + 1.84\rho \right] \quad (2)$$

Where  $\mu_0$  is the vacuum permeability,  $l_{avg}$  is the average strip length calculated over all the rings, and  $\rho$  is the so-called filling ratio.

$$l_{avg} = 4 \left[ l - (N-1)(u+s) \right] \quad (2.1)$$

$$\rho = (N-1)(u+s) / \left[ l - (N-1)(u+s) \right] \quad (2.2)$$

Using 2.1 and 2.2 we get,  $l_{avg}$  is 296nm and  $\rho$  is 0.081. Therefore, L is  $5.97 \times 10^{-13}$ H.

$$C = \frac{N-1}{2} \left[ 2l - (2N-1)(w+s) \right] C_0 \quad (3)$$

' $C_0$ ' is the per-unit-length capacitance between two parallel strips having width 'u' and separation 's' in the presence of a Dielectric substrate of height 'h' and relative permittivity ' $\epsilon_r$  sub' and is given by equation 3.1.

$$C_0 = \epsilon_0 \epsilon_r^{sub} \frac{K(\sqrt{1-k^2})}{K(k)} \quad (3.1)$$

Where  $\epsilon_0$  is the vacuum permittivity, 'K' is the complete elliptic integral of the first kind,  $k=s/(s+2u)$ , and ' $\epsilon_r$  sub' is the effective relative permittivity related to the dielectric filling the substrate is given by

$$\epsilon_r^{sub} = 1 + \frac{2}{\pi} \operatorname{artg} \left[ \frac{h}{2\pi(w+s)} \right] (\epsilon_r - 1) \quad (3.2)$$



Using above expressions we have found out,  $k=0.33$ ,  $K(k)=1.52$ ,  $K(1-k^2)^{0.5}=2.46$ ,  $\epsilon_{\text{sub}} = 1.134$ ,

$C_0=1.625 \times 10^{-11}$  F. Therefore, C is  $3.56 \times 10^{-18}$  F.

Resultant impedance of the circuit in Figure 6(b) is given by

$$Z = sL + R_1 + \frac{1}{sC + R_2} \quad (4)$$

Where  $s=j\omega$ , and  $\omega = 2\pi f$  where 'f' is the resonant frequency.

Frequency domain equivalent of Z is given by

$$Z = j\omega L + R_1 + \frac{1}{j\omega C + R_2} \quad (4.1)$$

At resonance, imaginary part of Z is zero. So,

$$j\omega L + \frac{j\omega C}{-\omega^2 C^2 - R_2^2} = 0$$

Neglecting  $R_2$ , we get

$$\omega = \sqrt{\frac{1}{LC}} \quad (5)$$

On substituting values of L and C we get, resonant frequency as 109THz.

Thus we find around 1% error between the simulational and analytical study of 4 segment SRR.

## 6. Designing of Metamaterial Embedded Antenna

Antenna is characterized by different parameters *e.g.*, gain, bandwidth, VSWR, 3dB beam width in E, H plane, and return loss. These parameters have been obtained for RMPA as in table 1 using HFSS. Parameter optimization using 4 segment SRR is done by embedding in the middle of the substrate SRR metamaterial in array of 6X5 elements spaced at  $dx=71.5\text{nm}$  and  $dy=75.3\text{nm}$  and center of the array coincides with the center of the antenna substrate just below the patch as shown in Figure 7.

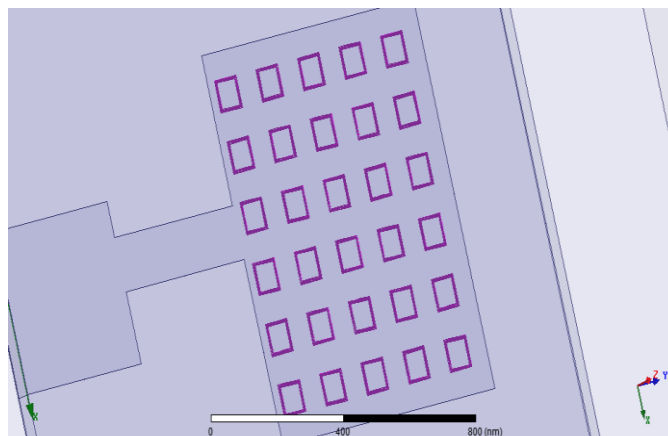
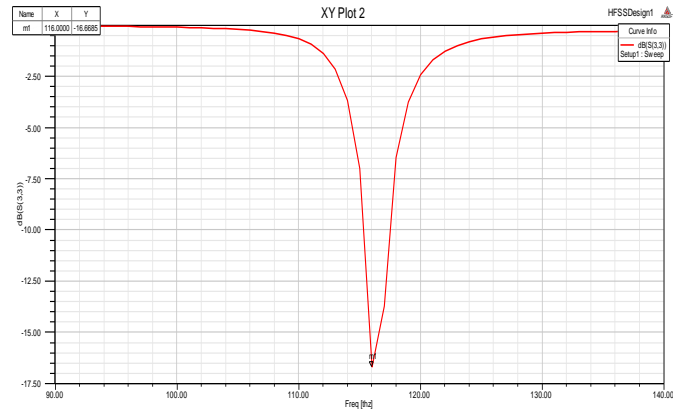
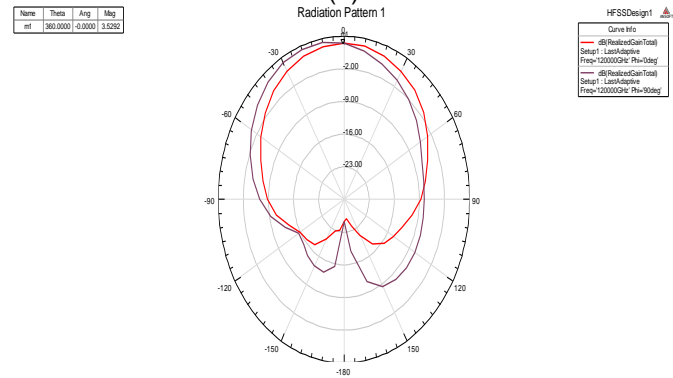


**Figure 7. Embedding 4 Segment SRR MTM Array Inside RMPA Substrate**

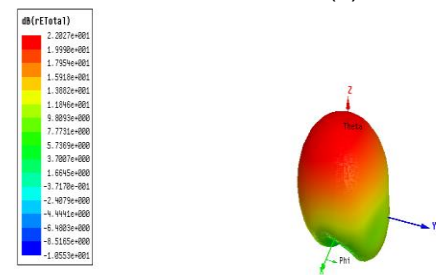
Simulation results for MTM array inside RMPA substrate are shown in Figure 8.



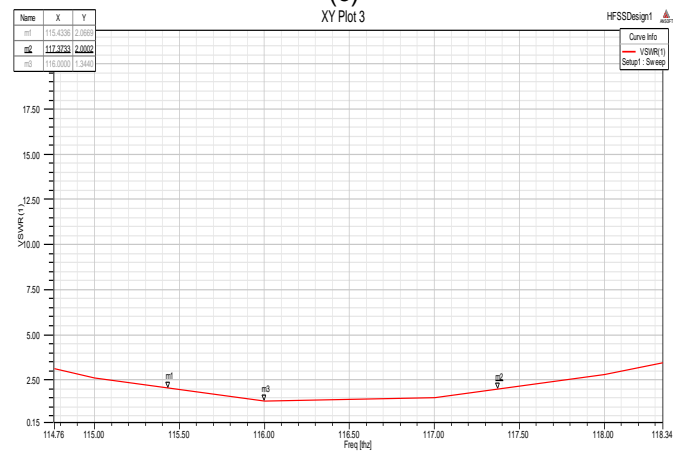
(a)



(b)



(c)



(d)

Figure 8. a) Return Loss b) E and H Radiation Pattern c) 3D Polar Plot d) VSWR

Table 4 gives the obtained simulated values of parameters and comparison of 4 Segment SRR MTM array RMPA with RMPA without MTM.

**Table 4. Simulation and Comparison Results of 4 Segment SRR MTM Array Embedded in RMPA Substrate**

ANTENNA/ Parameters	RMPA	RMPA with MTM	Improve ment (approx)
<b>S11 (dB)</b>	-19.86	-16.68	-19%
<b>VSWR</b>	1.23	1.34	-9%
<b>Bandwidth (THz)</b>	1.91	1.9397	1.6%
<b>H plane gain in dB</b>	3.6	3.5	-3%
<b>E plane gain in dB</b>	3.6	3.5	-3%
<b>Peak directivity(dB)</b>	5.9	6.01	2%
<b>Front to back lobe ratio</b>	32	35	9%

Each metamaterial cell can be considered as an independent resonating body having some resonant frequency. By placing new metamaterial, having same dimension, adjacent to previous one a 6 X 5 array has been formed. Thus, the resonating frequency 'f next' will affect 'f previous', thereby changing the equivalent frequency response. Thus, the change in the arrangement of unit cells will lead to change in parameters such as bandwidth, gain, VSWR.

## 7. Conclusion

This paper presents simulated results for a new signature – 4-segment SRR metamaterial unit cell structure and its application to a radiating patch antenna. It has been shown that the proposed structure exhibits negative values of  $\mu$  in the region of design-interest. When our proposed signature-4 segment SRR metamaterial structure is utilized to design a Rectangular Micro strip Patch Antenna an improvement of bandwidth by 30GHz, directivity by 2% and Front to back lobe ratio by 9% has been observed. However, gain decreases by 3% and return loss decreases by 19%. Trade off lies in improvement of above antenna parameters over gain and return loss. However, the coherence between equivalent circuit analysis using parametric study by applying CAD formulas in MATLAB and Finite Element Method technique in HFSS has been observed and is nearly about 15%.

## References

- [1] H. Chen, L. Ran, J. Huangfu, X. Zhang and K. Chen, "Left-handed materials composed of only S-shaped resonators", *Physical Review*, vol. 70, 057605, (2004).
- [2] A. Sihvola, "Character of surface plasmons in layered spherical structures", *PIER*, vol. 62, (2006), pp. 317-331.
- [3] [www.docstoc.com/docs/127876758/High-Frequency-Structure-Simulator-HFSS-Tutorial](http://www.docstoc.com/docs/127876758/High-Frequency-Structure-Simulator-HFSS-Tutorial)
- [4] C. A. Balanis, "Antenna Theory", John Wiley & Sons Inc, (1999).
- [5] 6x9 Handbook / Antenna Engineering Handbook / Volakis / 147574-5 / Chapter 7
- [6] V. G. Veselago, "The electrodynamics of substances with simultaneously negative values of  $\epsilon$  and  $\mu$ . *Soviet Physics-Uspeski*", vol. 10, no. 4, (1968) January-February, pp. 509-514.
- [7] J. B. Pendry, A. J. Holden, W. J. Stewart and I. Youngs, "Extremely low frequency plasmons in metallic micro structures", *Phys. Rev. Lett.*, vol. 76, (1996), pp. 4773-4776.
- [8] J. B. Pendry, A. J. Holden, D. J. Robbins and W. J. Stewart, "Magnetism from conductors and enhanced nonlinear phenomena", *IEEE Trans. Microwave Theory Tech.*, vol. 47, (1999) November, pp. 2075-2084.
- [9] D. R. Smith, W. J. Padilla, D. C. Vier, S. C. Nemat-Nasser and S. Schultz, "Composite Medium with Simultaneously Negative Permeability and Permittivity", *Physical Review Letters*, vol. 84, no. 18, (2000) May, pp. 4184-4187.

- [10] W. Withayachumnankul Derek Abbott, "Metamaterials in the Terahertz Regime", IEEE Photonics Journal, vol. 1, no. 2, (2009) August, pp. 99-118.
- [11] H. Benosman and N. Boukli Hacene, "Design and Simulation of Double "S" Shaped Metamaterial", IJCSI International Journal of Computer Science Issues, ISSN (Online): 1694-0814, vol. 9, issue 2, no. 1, (2012) March, pp. 534-537.
- [12] D. Ionescu and M. Kovaci, "About the Negative Permittivity of Some Metamaterial Composites - Simulational Study", IEEE 17th International Symposium for Design and Technology in Electronic Packaging (SIITME), (2011), pp. 197-200.
- [13] J. N. Li, W. Withayachumnankul, S. Chang and D. Abbott, "Practical method for determining inductance and capacitance of metamaterial resonators", Electronics Letters, vol. 48, no. 4, (2012), pp. 225-226.
- [14] Y. Minowa, M. Nagai, H. Tao, K. Fan, A. C. Strikwerda, X. Zhang, R. D. Averitt and K. Tanaka, "Extremely Thin metamaterial as slab waveguide at Terahertz frequencies", IEEE transactions on Terahertz Science and Technology, vol. 1, no. 2, (2011) November, pp. 441-449.
- [15] F. Bilotti, Senior Member, IEEE, A. Toscano, Member, IEEE, L. Vegni, Member, IEEE, K. Aydin, Student Member, IEEE, K. Boratay Alici and E. Ozbay, "Equivalent-Circuit Models for the Design of Metamaterials Based on Artificial Magnetic Inclusions", IEEE Transactions on Microwave Theory and Techniques", vol. 55, no. 12, (2007) December, pp. 2865-2873.
- [16] T. P. Weldon, R. S. Adams and R. K. Mulagada, "A Novel Unit Cell and Analysis for Epsilon Negative Metamaterial", IEEE, (2011), pp. 211-214.
- [17] E. Ekmekçi1 and G. Turhan-Sayan, "Investigation of effective permittivity and permeability of novel V shaped metamaterial using simulated S parameters", 5th International Conference on Electrical and Electronics Engineering, Bursa, Turkey, (2007).
- [18] H. S. Chen, L. X. Ran, J. T. Huangfu, X. M. Zhang and K. S. Chen, "Magnetic properties of S-shaped split-ring resonators", Progress In Electromagnetics Research, PIER, vol. 51, (2005), pp. 231-247.
- [19] Y. Minowa, M. Nagai, T. Hu, K. Fan, A. C. Strikwerda, X. Zhang, R. D. Averitt and K. Tanaka, "Extremely Thin metamaterial as slab waveguide at Terahertz frequencies", IEEE transactions on Terahertz Science and Technology, vol. 1, no. 2, (2011) November, pp. 441-449.
- [20] P. Dawar and A. De, "Bandwidth Enhancement of RMPA Using 2 Segment Labyrinth Metamaterial at THz", Materials Sciences and Applications, vol. 4, no. 10, (2013), pp. 579-588.
- [21] P. Dawar and A. De, "Tunability of Triangular SRR and Wire Strip (TSRR-WS) Metamaterial at THz", Advances in Optical Technologies, Article ID 405301, 10 pages, vol. 2014, (2014).
- [22] P. Dawar and A. De, "Bandwidth enhancement of RMPA using ENG metamaterials at THz", 2013 4th International Conference on Computer and Communication Technology (ICCCCT), 20-22 September, pp 11-16.